Cavity-enhanced frequency doubling from 795nm to 397.5nm ultra-violet coherent radiation with PPKTP crystals in the low pump power regime

Xin Wen, Yashuai Han, Jiandong Bai, Jun He, Yanhua Wang, Baodong Yang, and Junmin Wang*

State Key Laboratory of Quantum Optics and Quantum Optics Devices (Shanxi University), and Institute of Opto-Electronics, Shanxi University, 92 Wu Cheng Road, Tai Yuan 030006, Shan Xi Province, China
**wwjjmm@sxu.edu.cn*

Abstract: We demonstrate a simple, compact and cost-efficient diode laser pumped frequency doubling system at 795 nm in the low power regime. In two configurations, a bow-tie four-mirror ring enhancement cavity with a PPKTP crystal inside and a semi-monolithic PPKTP enhancement cavity, we obtain 397.5nm ultra-violet coherent radiation of 35mW and 47mW respectively with a mode-matched fundamental power of about 110mW, corresponding to a conversion efficiency of 32% and 41%. The low loss semi-monolithic cavity leads to the better results. The constructed ultra-violet coherent radiation has good power stability and beam quality, and the system has huge potential in quantum optics and cold atom physics.

OCIS codes: (190.2620) Harmonic generation and mixing; (140.4780) Optical resonators.

References and links

1. H. Guan, B. Guo, G. L. Huang, H. L. Shu, X. R. Huang, and K. L. Gao, "Stabalization of the 397nm and 866nm external cavity diode lasers for cooling a single calcium ion," Opt. Commun. **274**(1), 182–186 (2007).
2. N. M. Linke, C. J. Ballance, and D. M. Lucas, "Injection locking of two frequency-doubled lasers with 3.2 GHz offset for driving Raman transitions with low photon scattering in $^{43}Ca^{+}$," Opt. Lett. **38**(23), 5087–5089 (2013).
3. J. Appel, E. Figueroa, D. Korystov, M. Lobino, and A. I. Lvovsky, "Quantum memory for squeezed light," Phys. Rev. Lett. **100**(9), 093602 (2008).
4. F. Wolfgramm, A. Cerè, F. A. Beduini, A. Predojević, M. Koschorreck, and M. W. Mitchell, "Squeezed-light optical magnetometry," Phys. Rev. Lett. **105**(5), 053601 (2010).
5. X. J. Jia, Z. H. Yan, Z. Y. Duan, X. L. Su, H. Wang, C. D. Xie, and K. C. Peng, "Experimental realization of three-color entanglement at optical fiber communication and atomic storage wavelengths," Phys. Rev. Lett. **109**(25), 253604 (2012).
6. P. A. Franken, A. E. Hill, C. W. Peters, and G. Weinreich, "Genetation of optical harmonics," Phys. Rev. Lett. **7**(4), 118–119 (1961).
7. K. Hayasaka, Y. Zhang, and K. Kasai, "Generation of 22.8 mW single-frequency green light by frequency doubling of a 50-mW diode laser," Opt. Express **12**(15), 3567–3572 (2004).
8. Y. Y. Zhai, B. Fan, S. F. Yang, Y. Zhang, X. H. Qi, X. J. Zhou, and X. Z. Chen, "A tunable blue light source with narrow linewidth for cold atom experiments," Chin. Phys. Lett. **30**(4), 044209 (2013).
9. Y. S. Han, X. Wen, J. D. Bai, B. D. Yang, Y. H. Wang, J. He, and J. M. Wang, "Generation of 130mW of 397.5nm tunable laser via ring-cavity enhanced frequency doubling," J. Opt. Soc. Am. B **31**(8), 1942–1947 (2014).
10. I. Juwiler, A. Arie, A. Skliar, and G. Rosenman, "Efficient quasi-phase-matched frequency doubling with phase compensation by a wedged crystal in a standing-wave external cavity," Opt. Lett. **24**(17), 1236–1238 (1999).
11. I. Juwiler and A. Arie, "Efficient frequency doubling by a phase-compensated crystal in a semimonolithic cavity," Appl. Opt. **42**(36), 7163–7169 (2003).
12. S. Ast, R. M. Nia, A. Schönbeck, N. Lastzka, J. Steinlechner, T. Eberle, M. Mehmet, S. Steinlechner, and R. Schnabel, "High-efficiency frequency doubling of continuous-wave laser light," Opt. Lett. **36**(17), 3467–3469 (2011).
13. K. Schneider, S. Schiller, J. Mlynek, M. Bode, and I. Freitag, "1.1-W single-frequency 532-nm radiation by second-harmonic generation of a miniature Nd:YAG ring laser," Opt. Lett. **21**(24), 1999–2001 (1996).

#225849 - $15.00 USD Received 28 Oct 2014; revised 9 Dec 2014; accepted 14 Dec 2014; published 22 Dec 2014

14. X. Deng, J. Zhang, Y. C. Zhang, G. Li, and T. C. Zhang, "Generation of blue light at 426 nm by frequency doubling with a monolithic periodically poled $KTiOPO_4$," Opt. Express **21**(22), 25907–25911 (2013).
15. G. D. Boyd and D. A. Kleinman, "Parametric interaction of focused Gaussian light beams," J. Appl. Phys. **39**(8), 3597–3639 (1968).
16. W. Wiechmann, S. Kubota, T. Fukui, and H. Masuda, "Refractive-index temperature derivatives of potassium titanyl phosphate," Opt. Lett. **18**(15), 1208–1210 (1993).
17. R. W. P. Drever, J. L. Hall, F. V. Kowalski, J. Hough, G. M. Ford, A. J. Munley, and H. Ward, "Laser phase and frequency stabilization using an optical resonator," Appl. Phys. B **31**(2), 97–105 (1983).
18. R. L. Targat, J.-J. Zondy, and P. Lemonde, "75%-efficiency blue generation from an intracavity PPKTP frequency doubler," Opt. Commun. **247**(4-6), 471–481 (2005).
19. F. Villa, A. Chiummo, E. Giacobino, and A. Bramati, "High-efficiency blue-light generation with a ring cavity with periodically poled KTP," J. Opt. Soc. Am. B **24**(3), 576–580 (2007).
20. E. S. Polzik and H. J. Kimble, "Frequency doubling with $KNbO_3$ in an external cavity," Opt. Lett. **16**(18), 1400–1402 (1991).
21. G. K. Samanta, S. C. Kumar, M. Mathew, C. Canalias, V. Pasiskevicius, F. Laurell, and M. Ebrahim-Zadeh, "High-power, continuous-wave, second-harmonic generation at 532 nm in periodically poled $KTiOPO_4$," Opt. Lett. **33**(24), 2955–2957 (2008).
22. J. M. Yarborough, J. Falk, and C. B. Hitz, "Enhancement of optical second harmonic generation by utilizing the dispersion of air," Appl. Phys. Lett. **18**(3), 70–73 (1971).
23. R. Paschotta, P. Kürz, R. Heuking, S. Schiller, and J. Mlynek, "82% Efficient continuous-wave frequency doubling of 1.06 μm with a monolithic $MgO:LiMbO_3$ resonator," Opt. Lett. **19**, 1325–1327 (1994).
24. C. Zimmermann, R. Kallenbach, T. W. Hänsch, and J. Sandberg, "Doubly-resonant second-hermanic generation in β-barium-borate," Opt. Commun. **71**(3-4), 229–234 (1989).

1. Introduction

Ultra-violet (UV) laser has great potential in practical applications, like the laser printing and lithography, spectroscopy, quantum optics and other aspects in quantum physics. For instance, Ca^+ ion optical clock is treated as a potential frequency standard with its long lifetime of the $3D_{5/2}$ level. The 397nm laser, corresponding to the transition of Ca^+ $4S_{1/2}$-$4P_{1/2}$, can be used as the cooling laser in trapping the ions, plays an important part in the Ca^+ clock [1, 2]. Commercial lasers are now available in UV regime, but have limited output power and imperfect beam quality. In order to get lasers with better properties at such short wavelengths, the method of second harmonic generation (SHG) has been employed. These generated coherent radiation could be used to pump an optical parametric oscillator (OPO). The realized squeezed light, which is resonant on the atomic transition line, plays a significant role in quantum information processing. The squeezed light, with the variance of quantum fluctuations of one quadrature component dropping below the vacuum state, could act as the probe light to increase the signal to noise ratio and the sensitivity as well. Quantum memory has been realized using electromagnetically induced transparency in rubidium vapor cell with a pulsed squeezed vacuum [3]. The sensitivity of the magnetic field measurement can be improved with the squeezed light which indicates that this technic could be greatly used in such precise measurement fields [4]. An entangled source for the possible quantum network is accomplished with a cascaded nondegenerated OPO [5].

SHG was first demonstrated in 1961 [6]. In the experiment, they used a pulsed laser to observe the second harmonic (SH) at 347.2nm. As the generated SH power is quadratic to the incident fundamental laser, the majority of the frequency doubling experiments are undertaking in the high power regime, persuing higher power and efficiency. In the low power regime, the limited fundamental power leads to the low power density inside the cavity, but one can still get satisfying results. Kazuhiro Hayasaka *et al.* used a 50-mW extended-cavity diode laser at 1080nm and got a SH power of 22.8mW, the conversion efficiency was 51.6% [7]. However, the frequency doubling at 795nm is difficult, for the generated harmonic is in the UV regime, where the absorption is severe, and the optical elements are not always perfect because of the loss on the surfaces. Our 795nm SHG system is working with a maximum pump power of around 110mW to avoid the inevitable heating and we use a distributed-Bragg-reflector-type (DBR) diode laser as the pump source. Compared with the Ti: Sapphire laser or the tapered amplifier (TA), the diode laser is cost-

#225849 - $15.00 USD Received 28 Oct 2014; revised 9 Dec 2014; accepted 14 Dec 2014; published 22 Dec 2014

efficient and greatly improves the simplicity and compactness of the system. In addition, it will not destruct the beam quality like TA does.

Different frequency doubling configurations have been created to raise the power intensity in the nonlinear crystal to increase conversion efficiency. The most common configurations are bow-tie ring cavity, standing wave cavity, semi-monolithic cavity and the monolithic cavity. The bow-tie configuration, built up by four mirrors, has great flexibility but with much linear loss and a lack of stability. For the wavelength of rubidium D1 transition line at 795nm, Zhai *et al.* obtained 40mW UV coherent radiation at 397.5nm with a mode-matched fundamental power of 260mW [8]. Our group used a diode-pumped TA-boosted enhancement cavity with a periodically poled potassium titanyl phosphate (PPKTP) crystal, achieved a 130mW-output of 397.5nm coherent radiation, corresponding to an efficiency of 43% [9].The standing wave cavity reduces half of the mirrors and thus eliminates parts of the loss. A standing-wave cavity with a wedged PPKTP crystal got a second harmonic of 268mW and an efficiency of 69.4% [10].The last two cavity configurations have great difficulty in manufacturing, but could further reduce the linear loss, and could expect an increase in conversion efficiency. For the simi-monolithic doubler cavity, 117.5mW 532nm coherent radiation was achieved with a pump power of 208mW, the conversion efficiency was 56.5% [11]. 1.05W 775nm coherent radiation was obtained in a PPKTP crystal yielding an excellent efficiency of 95% [12]. About 1.1W 532nm coherent radiation was achieved in a plano-convex MgO:$LiNbO_3$ (MgO:LN) crystal, with an 89% efficiency [13]. In their experiment, they used a crystal with both faces polished flat and the end surface coated high-reflected as the cavity mirror. The efficiency was lowered by a factor of 2 compared with the plano-convex model. For the monolithic cavity, one need to control the temperature to realize the phase matching condition and maintain the cavity resonance, which is difficult to reach the equilibrium. A monolithic cavity was used to generate 426nm coherent radiation with a power of 158mW and a conversion efficiency of 45% [14]. As we perform the frequency doubling process in the low power regime, the linear loss of the cavities should be taken into good consideration. Here, we used two different kinds of cavities which have different loss level, studied the SHG in the low power regime.

Only a few works have presented the SHG at 397.5nm. The heavy absorption at this UV regime has greatly limited the conversion, so it is hard to get an excellent efficiency. Our previous work, listed as Ref [9], used a four-mirror bow-tie configuration with a diode-pumped TA-boosted pump source to process the SHG. With an amplified fundamental power to around 400mW, we were able to obtain larger SH power, the generated stable SH output could up to 130mW. However, the TA will break the spatial profile of the fundamental wave, which would lead to a poorer mode-matching condition. In this work, the DBR diode laser serves as the pump source, a bow-tie ring cavity (BRC) and a semi-monolithic cavity (SC) are used for frequency doubling, and the use of the low loss SC helped to enhance the nonlinear process. The generated UV coherent radiation with a-41%-conversion efficiency is satisfying at the low pump power regime.

2. Experimental setup

The schematic diagram of frequency doubling system is shown in Fig. 1. The pump source is a TO-8 packaged distributed-Bragg-reflector-type (DBR) diode laser at 795nm, with a typical line width of ~1MHz and a nominal maximum output power of 180mW. An optical isolator is placed in front of the doubling cavity to avoid the feedback to the pump laser, especially in the case of the semi-monolithic one. A phase-type electro-optical modulator (EOM) is used to generate a phase modulation to lock the cavity. A half wave plate is used to adjust the polarization of the pump laser to match with the crystal axis to get the maximum second harmonic generation.

The SC contains only an input mirror and a PPKTP crystal. The input coupler is a 30mm of radius of curvature mirror with a transmission of 5.6% at the fundamental wave laser (FW)

#225849 - $15.00 USD Received 28 Oct 2014; revised 9 Dec 2014; accepted 14 Dec 2014; published 22 Dec 2014

and a reflectivity larger than 99.5% at the second harmonic wave coherent radiation (SHW). The PPKTP crystal is plano-convex, and has a dimension of 1mm × 2mm × 10mm. The curved surface has a radius of 15mm and is coated yielding a reflectivity of about 99.5% at 795nm and a transmission of about 98.5% at 397.5nm, acting as the output coupler for the generated UV radiation. The plane surface is antireflection coated (the residual reflectivity is smaller than 0.2% for the FW and SHW). The input coupler and the crystal are separated for 26.8mm, in order to focus the beam waist at the center of the crystal and the waist is 43μm.

The configuration of the BRC consists of two plane mirrors (M1, M2) and two curved mirrors (M3, M4) with the radius of 100mm. The curved mirrors are separated for about 120mm, and the total cavity length is around 600mm with a folding angle of 8°, for which the astigmatism can be neglected. The PPKTP crystal is antireflection (the residual reflectivity is smaller than 0.2% for the FW and SHW) and has a dimension of 1mm × 2mm × 20mm. The crystal is mounted on a copper oven with a thermo-electric Peltier element to have the temperature stabilized. The waist of the fundemantal wave in the crystal is calculated to be 40μm. M1 acts as the input coupler with a transmission of 7.4% at the fundamental wavelength, other three mirrors are all coated a high reflector at 795nm, and the M4 has a transmission of 94% at the second harmonic wavelength. A piezo-electric transducer (PZT) is mounted on M2, which can be used to lock the cavity length.

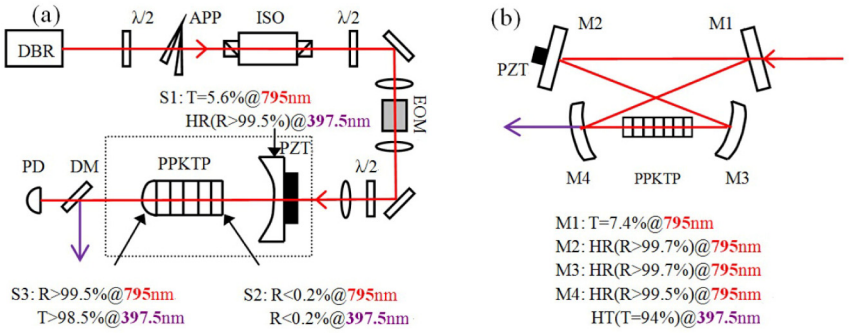

Fig. 1. Schematic diagram of the frequency doubling system. DBR: 795nm distributed- Bragg-reflector (DBR)-type diode laser; APP: anamorphic prism pair; ISO: optical isolator; EOM: phase-type electro-optical modulator; PZT: piezoelectric transducer; DM: dichroic mirror; PD: photo-diode. (a) The semi-monolithic cavity; (b) The bow-tie four-mirror ring cavity.

The frequency doubling crystal we choose is PPKTP. Owing to the technique of quasi-phase-matching (QPM), the crystal is periodically poled by the electric field with a proper grating period, so we are able to use the maximum nonlinear coefficient of the material. It is suitable for the SHG especially at low power regime. For the wavelength of 795nm, we use a crystal with the poling period of 3.15μm, corresponding to a phase matching temperature at about 50°C. The process of the SHG is noncritically phase matched by tuning the operating temperature. Both the FW and the SHW are close to the boundary of the transparent range of PPKTP (350nm - 4400nm), so the absorption here is severe, leading to a loss of the SH power and a thermal effect. To overcome the problem to the greatest degree, first we coat the end surface of the crystal high transmissible to the SH, so it propagates a single pass in the crystal, which helps to reduce the absorption. Then we use a loose focus condition. We choose the beam waist to be about 40μm, almost twice the optimal confocal condition as calculated from the Boyd and Kleinmann's theory [15], for theoretical optimal focusing parameter of $\xi = L/b = 2.84$, where L is the length of the crystal and $b = \pi\omega_0^2/\lambda$. The loose focus has only slight influence on the conversion, but will dramatically weaken the thermal effect, which will do good to the long-term stability of the cavity.

#225849 - $15.00 USD Received 28 Oct 2014; revised 9 Dec 2014; accepted 14 Dec 2014; published 22 Dec 2014

3. Results and discussion

We obtained the temperature tuning curve of both crystals, as shown in Fig. 2. The results match well with the sinc^2 function, indicating that the crystal is in good homogeneity of refraction index at such power level. For the semi-monolithic crystal, the phase-matching temperature is 53.0°C at the incident power of 140mW, and the full-width at half maximum bandwidth (FWHM) is 1.1°C. For a 100mW incident power, the phase matching temperature of the 20mm-long crystal is 50.5°C, and the FWHM is 0.5°C. The calculated phase matching temperature bandwidths are 1.0°C and 0.5°C respectively [16], proving the crystals have good quality.

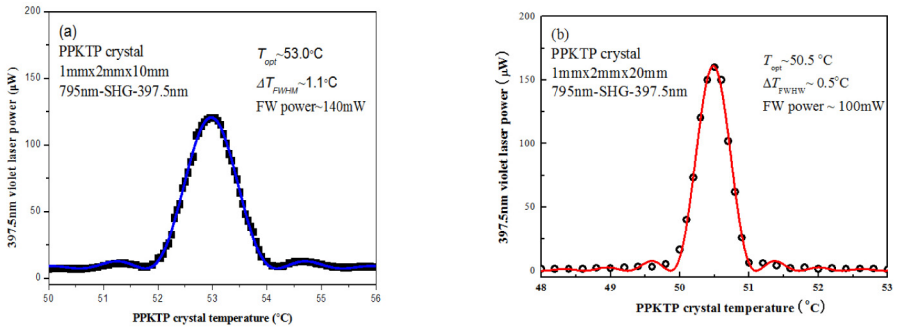

Fig. 2. The temperature tuning curves of the PPKTP crystals for single-pass frequency doubling from 795 nm to 397.5 nm. (a) 10mm-long PPKTP crystal; (b) 20mm-long PPKTP crystal.

The results of measured the SH power and the conversion efficiency versus the incident fundamental power are shown in Fig. 3. Squares and circles are the measured experimental data for the BRC and the SC respectively. Lines are calculated from the theory. For the BRC, with a mode-matched power of 110mW, we get an SH power of 35mW and a conversion efficiency of 32%. For the SC, output power and the conversion efficiency are 47mW and 41% respectively, when the mode-matched power is 115mW. The mode-matching efficiency of the BRC and the SC are 82% and 93% respectively. Each experimental point is carefully optimized by searching the phase matching temperature T_{opt} and the output power is measured when the cavity length is locked with a servo loop. We use the Pound Drever-Hall modulation sideband method to lock the cavity [17], with a modulation frequency of 4.1MHz. The cavity is locked with a good stability. The experiment results has been optimized with the transmission of the input coupler close to the calculated optimal ones, so that the coupling efficiency is reaching a satisfying condition.

The overall conversion efficiency can be written as a function of the mode-matched incident power [18,19]·

$$\sqrt{\eta}[2-\sqrt{1-T_1}(2-L-\Gamma\sqrt{\frac{\eta P_1}{E_{NL}}})]^2-4T_1\sqrt{E_{NL}P_1}=0 \qquad (1)$$

where $\eta = P_2/P_1$, is the overall efficiency, P_1 is the fundamental power, and P_2 is the generated SH power. L represents the round-trip loss except the transmission of the input coupler T_1. Here we fit the linear loss L in the BRC and the SC to be 4.4% and 2.5% respectively. Γ includes all nonlinear loss and is in the form of $\Gamma = E_{NL} + \Gamma_{abs}$, where Γ_{abs} means the absorption of the SH inside the crystal: $P_{abs} = \Gamma_{abs}P_c^2$, P_c is the circulating power in the resonant cavity. The measured absorption in blue region around 400nm is about 10%-20%/cm, as mentioned at [18, 19]. For the wavelength of 397.5nm, the absorption would be more severe, we assume $\Gamma_{abs} = 0.22E_{NL}$ in our model.

#225849 - $15.00 USD Received 28 Oct 2014; revised 9 Dec 2014; accepted 14 Dec 2014; published 22 Dec 2014

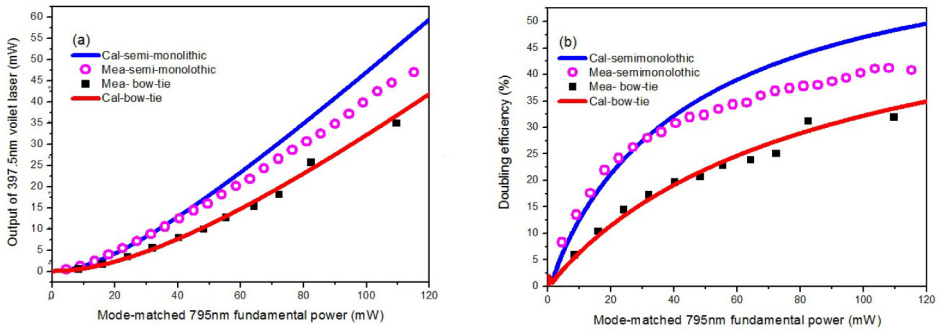

Fig. 3. (a) The SH power versus the mode-matched fundamental power. (b) The conversion efficiency versus the mode-matched fundamental power.

As we can see from the Fig. 3, the generated SH power and the conversion efficiency in the SC are higher than that in the BRC. It is because that in this configuration the intra-cavity loss is greatly reduced, for there is a cutback of the cavity mirrors and the crystal surfaces. On the other hand, the experimental results in the BRC match well with the calculated results, while in the SC show a deviation from the theory in higher power level. We attribute this phenomenon to the blue-induced thermal effect, including both blue-induced infrared absorption and the thermal lensing. Such effect will lead to a loss of the SH power and heat the crystal, especially in the SC. The FW and the residual SH propagate both forward and backward directions in the crystal and leading a more severe thermal loading. The heating will change the cavity length, form a thermal gradient inside the crystal and result in an asymmetry of the resonant signal, thus the deterioration of the error signal will make it hard to lock the cavity at the top of the peaks. The thermal lensing effect will add an inhomogeneity inside the crystal and destroy the previous focus condition. Changing the cavity length slightly will compensate for the deterioration to maintain a consistent SH power level [20]

The major influence of the thermal effect is on the stability of the SH power. The absorption at such short wavelength is so severe, thus the generated SH greatly heats the crystal, resulting in a bad thermal stability, especially in the SC. In this configuration, the frequency doubling crystal plays a more important role. The short cavity length is sensitive to the crystal length change caused by the heating-lead refractivity variation, and the thermal loading is more evident, which produce great difficulty in locking the cavity. The measured SH power stability is shown in Fig. 4. With an input fundamental power of around 110mW, we measure the output SH power for 30min. In the BRC, the RMS fluctuation is 0.7%, while in the SC, it is 1.9%. Despite the better mechanical stability of the SC, the fluctuation is still a bit larger. At this UV regime, thermal effect is the major limit to the stability of SH power. Further improvement could be made by enlarge the radius of the cured surface, so the beam waist could still be larger, one can use the loose focus to compensate part of the heating. For BRC, we can adjust the lengh between the two curved mirrors, shorter length will lead to a larger beam waist. For SC, we can replace the input coupler to a larger radius of curvature than the current one, and shorten or maintain the separated distance between the coupler and the plano surface of the crystal. A slight loose focus will not decrease much of the efficiency but will greatly reduce the thermal effect, and do good to the thermal stability of the cavity.

#225849 - $15.00 USD Received 28 Oct 2014; revised 9 Dec 2014; accepted 14 Dec 2014; published 22 Dec 2014

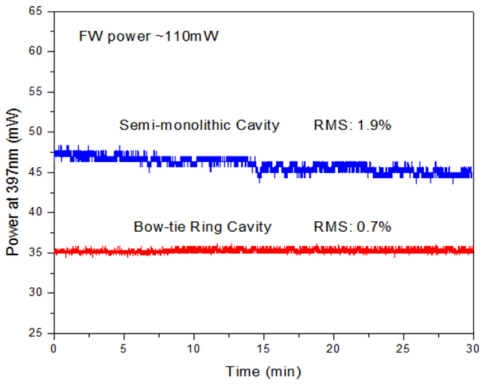

Fig. 4. Power stability of the SH output over 30min. The RMS fluctuations of the SC and the BRC are 1.9% and 0.7% respectively under the incident FW power of around 110mW.

We measured the beam quality M^2 of the generated UV coherent radiation. Results are shown in Fig. 5. (a) is for the SC, the measured M^2 of both axis are $M^2_x = 1.17$ and $M^2_y = 1.21$. (b) is for the BRC, they are $M^2_x = 1.19$ and $M^2_y = 1.16$.

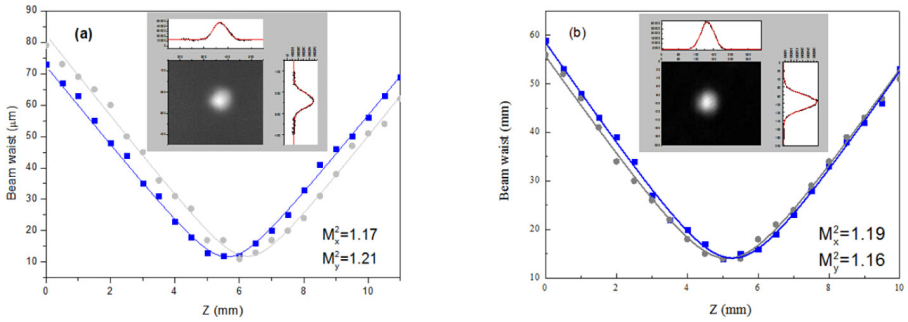

Fig. 5. The measured beam quality M^2 of the output UV coherent radiation. The blue squares are for the x axis, and the grey dots are for the y axis. The inserts are the beam profile of the SH. (a) is the result of SC, (b) is the result of BRC.

The tunability range of both fundamental wave and the second harmonic radiation is measured. By scanning the current of the DBR laser, we obtaine the saturation absorption spectroscopy of the Rb D1 line, which indicates that the fundamental wave can be tuned continuously around 8.5GHz. For the SHW, we use a confocal Fabry-Pérot cavity to monitor its modes. With the frequency doubling cavity locked, we scan the current of the DBR laser with a speed of 5.4GHz/s, the SHW can be tuned continuously around 3GHz which is limited by the deforming length of the PZT. We used the method of frequency beating to estimate the line width of the DBR diode laser, the measured instantaneous line width is around 1.3MHz, and the line width of the generated UV radiation should have the same order. Just as mentioned in Ref [21], G. K. Samanta *et al.* has measured the line widths of both the FW and SHW in their work, the obtained line widths are 12.5MHz and 8.5MHz respectively, the SHG process will not lead to an obvious change in line width.

Besides, we change the input coupler of the SC, which has a transmission larger than the calculated optimal one at the low power regime. It is used to qualitatively estimate the difference of linear loss between the two cavities. The frequency doubling crystal is working with the temperature tuned away from the phase matching one, so there is little nonlinear conversion. Figure 6 shows the resonant signals when the cavity length is scanned. (a) is for the SC, the finess is 40 when the transmission is 9.0%; (b) is the result of the BRC, the

#225849 - $15.00 USD Received 28 Oct 2014; revised 9 Dec 2014; accepted 14 Dec 2014; published 22 Dec 2014

calculated finess is 38 with the transmission of 7.4%. The resonant signals of both cavities indicate that the SC has less loss on the mirrors and the crystal surfaces, for it has higher finess even with larger transmission. We can contribute its higher doubling efficiency to the less linear loss.

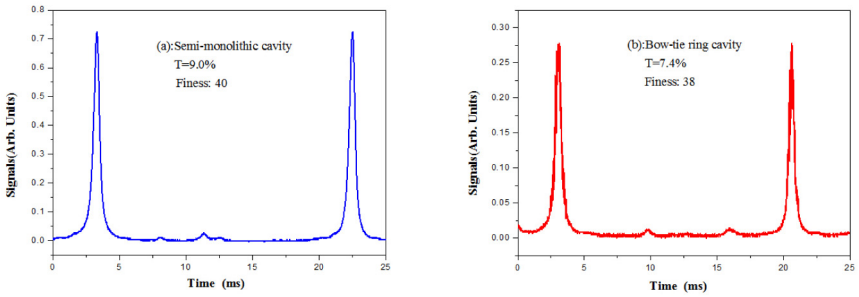

Fig. 6. The resonant signals of the cavities. The temperature is tuned away from the phase match condition. (a): The semi-monolithic cavity; (b): The bow-tie four-mirror ring cavity.

In the Fabry-Pérot cavity geometry (SC in our case), the phase matching condition deriving from the interference of the forward and backward waves leads to the modulation of the intracavity intensity. The constructed condition means that the relative phase is a multiple of 2π. Several methods have been applied to eliminate this kind of phase mismatching. Using a wedged crystal [10], utilizing the dispersion of air [22], adjusting the phase-matching temperature [23], and tilting the birefringent crystal [24] are all the feasible ways to compensate the phase mismatching. These methods could be utilized to further improve our experiments.

4. Conclusion

In conclusion, benefiting from the compact, convenient and inexpensive of the diode laser, we demonstrate the UV frequency doubling system at the low power regime. We use a bow-tie ring enhancement cavity and a semi-monolithic doubler respectively, using a loose focus condition to compensate part of the absorption caused thermal effect. The generated SH has a stable power output in the 30-min range, and has a good beam quality which is consistent with the Gaussian profile. In the SC, we obtain a stable SH radiation of 47mW and a conversion efficiency of 41% with a mode-matched fundamental power of 115mW, which is higher than that in the bow-tie configuration. Such SC is more suitable for these loss sensitive nonlinear transitions, both the second harmonic generation and the following process of OPO. In the low power regime, the generated SH power is limited by the intra-cavity loss, which could be improved by using the super polished mirrors with high quality coating. A modified display of the cavity could be expected to improve the long term power stability of the output SH.

The SHG process gives us the access to the coherent radiation at short wavelengths, especially the UV regime. The realized UV coherent radiation usually has better beam quality and satisfying power, so it could be useful in quantum physics. For instance, pumping the subthreshold OPO and producing squeezed vacuum. The generated squeezed light will be effective in fields like the precise measurements and spectroscopy.

Acknowledgments

This project is supported by the National Natural Science Foundation of China (grant nos. 61227902, 61475091, 11274213, 61205215, and 11104172), the National Major Scientific Research Program of China (grant no. 2012CB921601), and the Project for Excellent Research Team from the National Natural Science Foundation of China (grant no. 61121064).